

# Isolated Bidirectional Converter With High Voltage Gain Using Fixed Frequency Variable Amplitude Modulation Technique

Navaneetha Krishnan. J<sup>1</sup>, Sam Stanley. R<sup>2</sup>, Pavalarajan. S<sup>3</sup>

<sup>1,2</sup>Dept of Electrical and Electronics Engineering

<sup>3</sup>Dept of Information and Technology

<sup>1,2</sup>Christian College of Engg. & Tech, Dindigul, India.

<sup>3</sup>PSNA College of Engg. & Tech, Dindigul, India.

**Abstract-** This paper proposes a bidirectional three-level LLC resonant converter with a new pulse width and amplitude modulation control method. With different control signals, it has three different operation modes with different voltage gains. Therefore, it can achieve wide voltage gain range by switching among these three modes, which is attractive for energy storage system applications needing wide voltage variation. The proposed topology operates with constant switching frequency, which is easy to implement with digital control, and it can achieve soft switching for all the switches and diodes in the circuit as a conventional LLC resonant converter. The performance of the proposed converter is validated by the experimental results from a 1-kW prototype with 20 A maximum output current.

**Keywords-** Bidirectional, constant switching frequency, LLC, three-level (TL), wide voltage gain.

## I. INTRODUCTION

More and more research efforts have been focused on how to use the clean energy in an efficient way in recent years for energy saving and environment protection. The distributed generation systems (DGSs) with clean renewable energy resources like photovoltaic, wind power, and fuel cell are widely adopted around the world. However, the intermittent nature of these clean renewable energy resources may cause fluctuation between power generation and consumption [1], [2]. So energy storage systems (ESSs) are required in DGSs to deal with the intermittent outages and make the system more stable and reliable. Batteries and super capacitors are the most popular energy storage components considering the price and performance. Fig. 1 shows a typical DGS with renewable energy resources and ESSs. The ESSs should have bidirectional power flow capability to store the excess energy generated by renewable resources, and release it when the load is heavy or renewable energy is not sufficient [3], [4]. The bidirectional dc–dc converter is a key component in ESSs to enable the bidirectional power flow. Galvanic

isolation is usually required for safety consideration. Besides, voltage variation of both the renewable energy resources and energy storage components is wide, so the voltage gain range of the bidirectional dc–dc converter should be as wide as possible.

Many isolated bidirectional topologies have been proposed and studied in recent years, and the dual-active-bridge converter is one of the most popular topologies for its simplicity and high power density [5]–[19]. However, it suffers from high circulating energy and high turn-off power loss. A lot of control methods have proposed to minimize the circulating energy or extend its soft-switching range by phase shift or duty cycle control, but the control methods are complex and cannot solve all the disadvantages at the same time [12]–[18].

In order to further improve the efficiency, an LLC resonant converter is a promising candidate. It can achieve soft switching for all the power devices and its efficiency is quite high [19]–[22]. A bidirectional LLC resonant topology for vehicular applications was proposed in [23]. The topology was still a traditional SRC during backward operation, which can only operate under buck mode. In [24], a symmetrical bidirectional CLLC resonant converter with two resonant tanks was proposed. The extra resonant tank increased both the cost and volume of the converter, and the voltage gain was reduced compared with the traditional LLC converter especially at heavy-load condition. Furthermore, forward mode and backward mode cannot be switched automatically, and the current in the output side has to flow through the body diodes of the switches which may cause high conduction loss. A bidirectional LLC resonant converter with an auxiliary inductor is proposed in [25], which has a symmetrical structure in forward mode and backward mode, and it can automatically change the power flow direction by simply regulating the switching frequency. However, the voltage gain is still limited for reasonable conversion efficiency and switching frequency variation range.

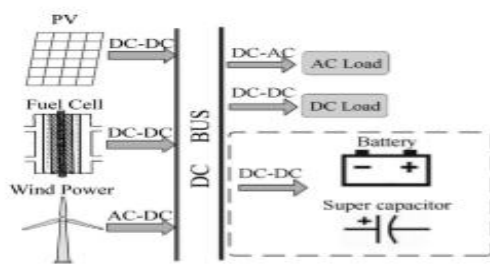


Fig. 1. Typical DG system with ESSs

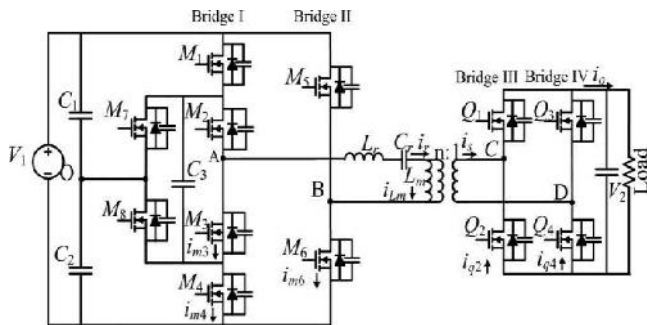


Fig. 2. Proposed bidirectional TL LLC resonant converter

voltage gain or light-load condition [26]–[31]. In [32] and [33], soft switching can always be achieved with extra components, which increases cost and complexity. A unidirectional three-level (TL) constant-frequency LLC resonant converter with hybrid full-bridge structure is proposed in [34] to achieve wider voltage gain range. However, duty cycle has to be very small in low voltage gain condition, the ZVS will be lost and the conduction loss is high due to small duty cycle.

To further improve the performance of a bidirectional LLC resonant converter, this paper proposes a TL LLC converter with a pulse width and amplitude modulation (PWAM) control method. The switching frequency is constant and equal to its resonant frequency, thus the converter can achieve soft switching for all switches easily. With three different control schemes, the converter can achieve a wide voltage gain.

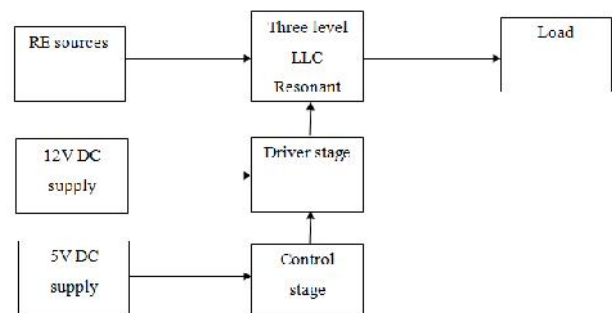
The proposed bidirectional TL LLC resonant converter is shown in Fig. 2, which has a hybrid full-bridge structure with MOSFETS M1 –M6 in the transformer primary side and a full-bridge structure with MOSFETS Q1 –Q4 in the secondary side, D1 and D2 are the body diodes of Q1 and Q2 , D5 –D8 are the body diodes of MOSFET M5 –M8 , respectively. MOSFETS M1 to M4 are connected in series to form a TL switching leg I, M5 and M6 are series connected to form bridge leg II. “A” and “B” are the midpoints of bridge leg I and II. “C” and “D” are the

midpoints of secondary-side full bridge. n is the transformer turns ratio. In order to achieve bidirectional power flow, MOSFETS M7 and M8 are used as clamp switches instead of conventional clamp diodes. The input source V1 is in the transformer primary side, while the energy storage element V2 is in the transformer secondary side. Lr is the resonant inductor, Cr is the resonant capacitor, and Lm is the magnetizing inductor of the transformer. Capacitor C3 is the flying capacitor.

The operation principle in forward mode and backward mode are analyzed in Section II and Section III, respectively. Section IV presents the performance analysis and design considerations for the proposed bidirectional LLC converter. A prototype with maximum 20-A output current is built and the experiments results are given in Section V. To simplify the steady-state analysis, some assumptions are given as follows:

1. All the MOSFETS with their body diodes and all the passive components are ideal, the dead time between switching signals are neglected;
2. Output capacitor Co is large enough and the output volt-age V2 is constant; C1 and C2 are also large enough, the voltage ripple can be neglected, and the dc voltage across them is 0.5 V1 ;
3. Co ss1 –Co ss8 are the parasitic capacitors of M1 – M8 , which have the same capacitance Co ss ; the parasitic capacitors of Q1 –Q4 also have the same capacitance Coss referred to the transformer primary side;
4. Current of the MOSFET is assumed to be constant during its ON/OFF transient.

## II. BLOCK DIAGRAM



Renewable energy is generally defined as energy that is collected from resources which are naturally replenished on a human timescale, such as sunlight, wind, rain, tides, waves, and geothermal heat. Renewable energy resources exist over

wide geographical areas, in contrast to other energy sources, which are concentrated in a limited number of countries.

Renewable energy is the energy which comes from natural resources such as sunlight, wind, rain, tides and geothermal heat. These resources are renewable and can be naturally replenished. Therefore, for all practical purposes, these resources can be considered to be inexhaustible, unlike dwindling conventional fossil fuels. Clean Development Mechanisms (CDMs) are being adopted by organizations all across the globe.

The major factor working against fossil fuels is the pollution associated with their combustion. Contrastingly, these sources are known to be much cleaner and produce energy without the harmful effects of pollution unlike their conventional counterparts.

Current day turbines range from around 600kW to 5MW of rated power. Since the power output is a function of the cube of the wind speed, it increases rapidly with an increase in available wind velocity. Recent advancements have led to aerofoil wind turbines, which are more efficient due to a better structure.

The tapping of solar energy owes its origins to the British astronomer John Herschel who famously used a solar thermal collector box to cook food during an expedition to Africa. Solar energy can be utilized in two major ways. Firstly, the captured heat can be used as solar thermal energy, with applications in space heating. Another alternative is the conversion of incident solar radiation to electrical energy, which is the most usable form of energy. This can be achieved with the help of solar photovoltaic cells or with concentrating solar power plants.

Hydropower installations up to 10MW are considered as small hydropower and counted as renewable energy sources. These involve converting the potential energy of water stored in dams into usable electrical energy through the use of water turbines. Run-of-the-river hydroelectricity aims to utilize the kinetic energy of water without the need of building reservoirs or dams.

Plants capture the energy of the sun through the process of photosynthesis. On combustion, these plants release the trapped energy. This way, biomass works as a natural battery to store the sun's energy and yield it on requirement.

Geothermal energy is the thermal energy which is generated and stored within the layers of the Earth. The gradient thus developed gives rise to a continuous conduction of heat from the core to the surface of the earth. This gradient

can be utilized to heat water to produce superheated steam and use it to run steam turbines to generate electricity.

The current trend across developed economies tips the scale in favour of Renewable Energy. For the last three years, the continents of North America and Europe have embraced more renewable power capacity as compared to conventional power capacity. Renewable accounted for 60% of the newly installed power capacity in Europe in 2009 and nearly 20% of the annual power production.

The Dual Active Bridge (DAB) converter is popular amongst researchers over the past two decades. High performance, high efficiency along with soft switching capability and galvanic isolation are notable benefits of this converter topology.

A driver is an electrical circuit or other electronic component used to control another circuit or component. They are usually used to regulate current flowing through a circuit or to control other factors such as other components, some devices in the circuit. Here 12V DC supply is given to the driver stage. 5V DC supply is given to control stage. These driver stage and control stage are used to give the gate pulses to the MOSFETs in converter.

### III. FORWARD MODE OPERATION

When the converter is in forward mode operation, the MOS-FETs in the primary side can be divided into three pairs: M1 and M4, M2 and M3, and M5 and M6. MOSFETs in each pair turn ON and OFF complementary. M7 and M8 are always OFF and their body diodes are used to clamp the voltage of M1 –M4 to half of the input voltage. Q1 –Q4 form the rectifier circuit in the secondary side. Since the voltage drop on MOSFETs' body diodes is high, Q3 and Q4 are used as synchronous rectifier to reduce the conduction loss, while Q1 and Q2 are always OFF to ensure DCM operation.

VA B is the voltage across point "A" and "B", and the equivalent ac voltage of VA B is applied to the resonant tank, and the output voltage is determined by its amplitude and pulse width. Since the switching frequency is constant, duty cycle and phase shift angles between different pairs of MOSFETs are used to regulate the amplitude and pulse width of VA B, so the pro-posed control method is a kind of PWAM method. With PWAM control, the amplitude of VA B will be different based on the ON/OFF status of M1 –M6.

#### High Gain (HG) Mode

The peak-to-peak amplitude of  $V_{AB}$  shown in Fig. 3(a) is  $2V_1$ , which is the highest one and the output voltage gain will also be the highest, so it is called the HG mode. Duty cycle of M1 and M3 is equal to  $\alpha$ , and  $\alpha$  is the control variable in HG mode to regulate the output voltage. The duty cycle of M5 and M6 is always 0.5. The phase shift time between M1/M4 and M3/M2 is always equal to  $0.5T_s$ . The switching frequency is fixed to the resonant frequency  $f_r$  formed by  $L_r$  and  $C_r$ , i.e.,  $T_s = 1/f_r$ . There are six stages in one switching cycle  $T_s$ , and the corresponding equivalent circuits of the first-half switching cycle are shown in Fig. 4(a)–(c).

**Stage 1 ( $t_0$ – $t_1$ ):** In this stage, M1, M2, and M6 in the primary side and Q1's body diode D1 and Q4 in the secondary side are ON. The resonant current  $i_r$  is negative and equal to the magnetizing current  $i_{Lm}$  at  $t_0$ , and it increases in a resonant mode during this stage. Stage 2 ( $t_1$ – $t_2$ ): M1 turns OFF and M4 turns ON at  $t_1$ , while M2, M6, D1, and Q4 keep ON during this stage.  $V_{AB}$  is equal to  $0.5V_1$ . Since the resonant current  $i_r$  is above zero, it will charge the parasitic capacitor of M1 until it reaches  $0.5V_1$ , and M4 can turn ON with ZVS. Voltage of the flying capacitor C3 is clamped to  $0.5V_1$  through the body diode of M7. As soon as  $i_r$  equals to  $i_{Lm}$  at  $t_2$ , this stage ends. Stage 3 ( $t_2$ – $t_3$ ): Once  $i_r$  is equal to  $i_{Lm}$  at  $t_2$ , the current through D1 is zero and it turns OFF with ZCS, the converter goes into DCM operation. Since Q1 is always OFF, the current will not reverse during this mode. The equivalent circuit is shown in Fig. 4(c). The secondary side is separated from the primary side, and load is supplied by the output capacitor.  $L_r$ ,  $L_m$ , and  $C_r$  form the resonant tank. Since  $L_m$  is much larger than  $L_r$ , the resonant period is quite long and the resonant current decreases slowly. This stage ends when M2 and M6 turn OFF at  $t_3$ , and M3 and M5 can turn ON with ZVS in the next stage. In the next half switching cycle, the operation principle of stages 4–6 is similar to stages 1–3 except the current direction is changed, which is not repeated here.

### Medium Gain (MG) Mode

The peak-to-peak amplitude of  $V_{AB}$  shown in Fig. 3(b) is equal to  $1.5V_1$  and its voltage gain will be lower than the HG mode, so it is called the MG mode. In MG mode,  $V_{AB}$  is equal to  $V_1$ ,  $0.5V_1$ ,  $-0.5V_1$  and 0 in different stages in a switching cycle, so it is asymmetrical, and the average dc value of  $V_{AB}$  is equal to  $0.25V_1$ , which is blocked by the resonant capacitor  $C_r$  and will not affect the operation of converter. The equivalent ac voltage applied to the resonant tank is also a symmetrical TL voltage. The time duration of  $V_{AB} = V_1$  in a switching period is  $T_s$ , and  $\alpha$  is the phase shift angle between M4/M3 and M6, which is used to regulate the output voltage in MG mode. Due to the asymmetrical

voltage waveforms of  $V_{AB}$ , the control signals for the MOSFETs are also asymmetrical, which makes the energy flow through C1, C2, and C3 unbalanced in a switching cycle. In order to solve this problem, the energy flow through the capacitors should be in opposite direction in next switching cycle, thus the energy can be balanced in two consecutive switching cycles. For example, if the capacitors are charged in the first switching cycle, it should be discharged in the next cycle, and vice versa. Therefore, the switching frequency  $f_e$  for M1–M4 is half the resonant frequency  $f_r$ . It should be known that the switching frequency of M5/M6 and Q3–Q4 is still equal to the resonant frequency.

There are 12 operation stages in an equivalent switching period. Stage 1 ( $t_0$ – $t_1$ ): M1, M2, M6, D1, and Q4 conduct in this stage, and the equivalent circuit is shown in Fig. 4(a), which is exactly the same as Stage 1 in HG mode. Stage 2 ( $t_1$ – $t_2$ ): M2, M4, and M6 conduct in this stage, which is also same as stage 2 in HG mode. The equivalent circuit is shown in Fig. 4(b). Since  $i_r$  is above zero, C3 will be discharged in this stage. Stage 3 ( $t_2$ – $t_3$ ): When  $i_r$  equals to  $i_{Lm}$  at  $t_2$ , the converter is in DCM operation, which is same as stage 3 in HG mode. The equivalent circuit is shown in Fig. 4(c). Stage 4 ( $t_3$ – $t_4$ ): M2, M4, and M5 in the primary side and Q2's body diode and Q3 in the secondary side conduct in this stage.  $V_{AB} = -0.5V_1$ , and the equivalent circuit is shown in Fig. 4(d). The resonant current  $i_r$  is positive at  $t_3$  and will decrease to negative during this stage. So C3 will be discharged at first and then it will be charged. Stage 5 ( $t_4$ – $t_5$ ): M4 turns OFF and M1 turns ON at  $t_4$ .  $V_{AB} = 0$ , and the equivalent circuit is shown in Fig. 4(e). The resonant current decreases to the magnetizing current  $i_{Lm}$ , the secondary side keeps the same as previous stage. Stage 6 ( $t_5$ – $t_6$ ): Once  $i_r$  is equal to  $i_{Lm}$ , the secondary-side switches are all OFF, and the converter is in DCM operation. The equivalent circuit is shown in Fig. 4(f). Stage 7 ( $t_6$ – $t_7$ ): M5 turns OFF and M6 turns ON, the equivalent circuit of stage 7 is same as stage 1 as shown in Fig. 4(a). Stage 8 ( $t_7$ – $t_8$ ): M1, M3, M6 in the primary side and Q1's body diodes and Q4 in the secondary side conduct.  $V_{AB} = 0.5V_1$ , the equivalent circuit is shown in Fig. 4(g). Since the resonant current  $i_r$  is positive, C3 will be charged. The amplitude of  $i_r$  in stage 2 and stage 8 are same, so the charger variation of C3 during these two stages is also equal, which can be balanced automatically. Stage 9 ( $t_8$ – $t_9$ ): Once  $i_r$  is equal to  $i_{Lm}$ , the converter is in DCM operation. The equivalent circuit is shown in Fig. 4(h). Stage 10 ( $t_9$ – $t_{10}$ ): M1 and M3 keep ON, M6 turns OFF and M5 turns ON in this stage, and the equivalent circuit is shown in Fig. 4(i). The resonant current  $i_r$  is positive at  $t_9$ , so C3 will be charged first. Then,  $i_r$  drops to negative and C3 is discharged. Energy flow through C1–C3 is in opposite direction during stage 4 and stage 10, so it can be balanced. Stage 11 ( $t_{10}$ – $t_{11}$ ): M1, M2,

M5, and Q3 are ON. The operation principle in stage 11 is same as stage 5, and the equivalent is shown in Fig. 4(e). The resonant current decreases to  $i_{Lm}$ . Stage 12 ( $t_{11}$ – $t_{12}$ ): Once  $i_r$  is equal to  $i_{Lm}$ , the converter is in DCM operation. The operation in stage 12 is same as stage 6. As a conclusion, by adopting the asymmetrical control method, energy of the capacitors C1–C3 can always be balanced. Since the switching frequency of M1–M4 is half the resonant frequency, the switching loss will also reduce. ZVS can always be achieved for M1–M6 and ZCS is achieved for Q1–Q4.

**IV. BACKWARD MODE OPERATION**

When the converter is in backward mode operation, the trans-former secondary side is the input side. The operation of the converter is similar to a series resonant converter, and the maximum voltage gain is 1.

There are also three operation modes as that in forward mode operation: HG mode, MG mode, and LG mode according to different control schemes. Key waveforms and control schemes. of three different modes are shown in Fig. 5. Switching frequency of Q1 –Q4 is equal to the resonant frequency. M5 and M6 are always OFF, and their body diodes are used as rectifier in backward operation. Similar to that in forward operation, the switching frequency of M1 –M4 is equal to the resonant frequency in HG mode and LG mode, and it will be equal to half the resonant frequency in MG mode.

**V. SIMULATION**

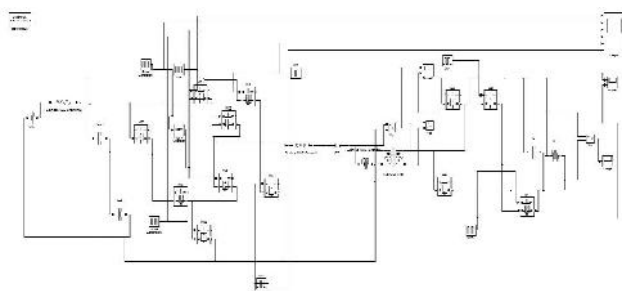


**Fig. 3.Simulation Diagram**

Input dc source is given to the circuit. The ripples may present in the input source. To reduce this ripples capacitors C1, C2 are used. These capacitors are used as a filter capacitors. Then the dc source is given to the MOSFET's

M1 to M2. These MOSFETs are acts as a rectifiers. These are used to give a dc source in squared wave. The step down transformer reduced the given input source. Then the

reduced dc source is given to the inverter. It converts dc to ac source. Then this ac source is given to the load.

**VI. RESULT**

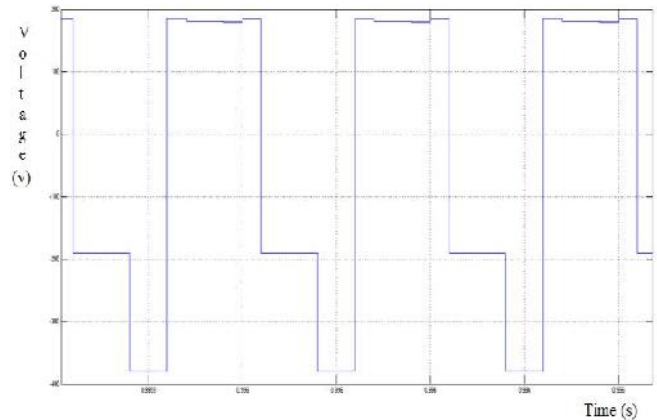


**Fig 4. Input voltage**

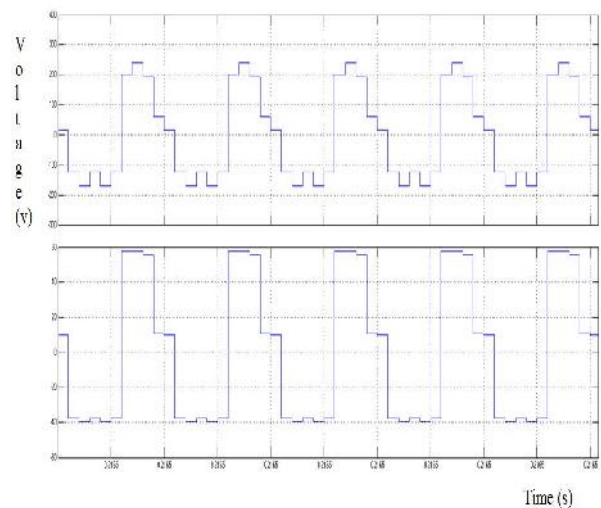


**Fig : 5 Comparison of input and output voltages**

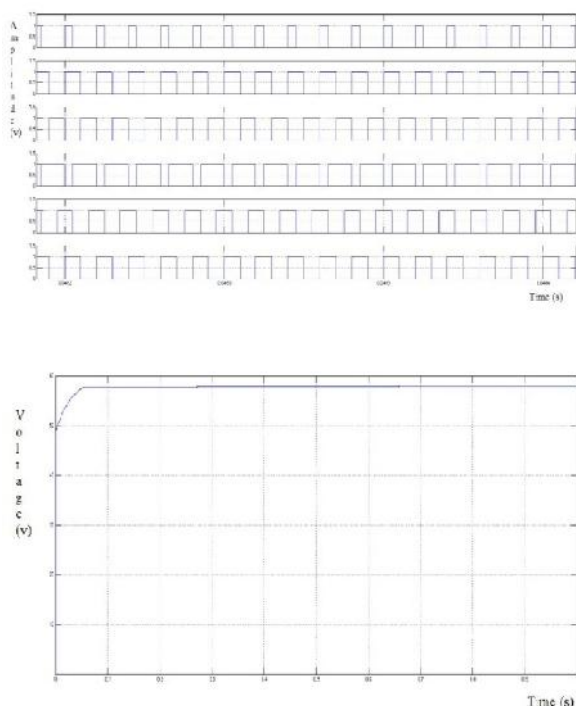


**Fig :6 Moefet and Output voltage**

## VII. CONCLUSION

This paper proposes a bidirectional TL LLC resonant converter with a new PWAM control strategies. The switching frequency is fixed to the resonant frequency and the equivalent amplitude of the voltage is regulated to control the output. With different control schemes, a very wide voltage gain range can be achieved, which overcomes the narrow voltage gain limitation of a conventional LLC resonant converter. Bidirectional operation can also be achieved with the proposed control method, and the operation principle in forward mode and backward mode is symmetrical. Finally, a 1-kW prototype is built and verifies the theoretical analysis.

## REFERENCES

- [1] H. Kakigano, Y. Miura, and T. Ise, "DC micro grid for super high quality distribution-system configuration and control of distributed generations and energy storage devices," in Proc. IEEE Power Electron. Spec. Conf., 2006, pp. 3148–3154.
- [2] A. Q. Huang, M. L. Crow, G. T. Heydt, J. P. Zheng, and S. J. Dale, "The future renewable electric energy delivery and management system: the energy internet," Proc. IEEE, vol. 99, no. 1, pp. 133–148, Jan. 2011.
- [3] M. Liserre, T. Sauter, and J. Hung, "Future energy systems: Integrating renewable energy sources into the smart power grid through industrial electronics," IEEE Trans. Ind. Electron., vol. 4, no. 1, pp. 18–37, Mar. 2010.
- [4] X. She, A. Q. Huang, S. Lukic, and M. E. Baran, "On integration of solid state transformer with zonal DC microgrid," IEEE Trans. Smart Grid, vol. 2, no. 3, pp. 975–985, Jun. 2012.
- [5] F. Z. Peng, H. Li, G.-J. Su, and J. S. Lawler, "A new ZVS bidirectional DC-DC converter for fuel cell and battery application," IEEE Trans. Power Electron., vol. 19, no. 1, pp. 54–65, Jan. 2004.
- [6] J. Lee, J. Jo, S. Choi, and S.-B. Han, "A 10-kW SOFC low-voltage battery hybrid power conditioning system for residential use," IEEE Trans. Energy Convers., vol. 21, no. 2, pp. 575 – 585, Jun. 2006.
- [7] B.-Y. Choi, Y.-S. Noh, Y.-H. Ji, B.-K. Lee, and C.-Y. Won, "Battery-integrated power optimizer for PV-battery hybrid power generation system," in Proc. IEEE Veh. Power Propulsion Conf., 2012, pp. 1343–1348.
- [8] J. A. Sabate, V. Vlatkovic, R. B. Ridley, F. C. Lee, and B. H. Chon, "De-sign considerations for high-voltage high-power full-bridge zero-voltage-switched PWM converter," in Proc. Appl. Power Electron. Conf., 1990, pp. 275–284.
- [9] M. H. Kheraluwala, R.W. Gascoigne, D. M. Divan, and E. D. Baumann, "A three-phase soft-switched high-power-density dc/dc converter for high-power application," IEEE Trans. Ind. App., vol. 27, no. 1, pp. 63–73, Jan./Feb. 1991.
- [10] S. Inoue and H. Akagi, "A bidirectional dc-dc converter for an energy storage system with galvanic isolation," IEEE Trans. Power Electron., vol. 22, no. 6, pp. 2299–2306, Nov. 2007.
- [11] F. Krismer and J. W. Kolar, "Accurate small-signal model for the digital control of an automotive bidirectional dual active bridge," IEEE Trans. Power Electron., vol. 24, no. 12, pp. 2756–2768, Dec. 2009.
- [12] F. Krismer and J. W. Kolar, "Efficiency-optimized high-current dual active bridge converter for automotive applications," IEEE Trans. Power Electron., vol. 59, no. 7, pp. 2745–2760, Jul. 2012.
- [13] G. G. Oggier, G. O. Garcia, and A. R. Oliva, "Modulation strategy to operate the dual active bridge dc-dc converter under soft-switching in the whole operating range," IEEE Trans. Power Electron., vol. 26, no. 4, pp. 1228–1236, Apr. 2011.
- [14] B. Zhao, Q. Song, and W. Liu, "Efficiency characterization and optimization of isolated bidirectional DC-DC converter based on dual-phase-shift control for DC distribution application," IEEE Trans. Power Electron., vol. 28, no. 4, pp. 1711–1727, Apr. 2013.
- [15] H. Bai and C. Mi, "Eliminate reactive power and increase system efficiency of isolated bidirectional dual-active-bridge DC-DC converter using novel dual-phase-shift

- control,” *IEEE Trans. Power Electron.*, vol. 23, no. 6, pp. 2905–2914, Nov. 2008.
- [15] D. Constinett, D. Maksimovic, and R. Zane, “Design and control for high efficiency in high step-down dual active bridge converters operating at high switching frequency,” *IEEE Trans. Power Electron.*, vol. 28, no. 83931–3940, Aug. 2013.
- [16] X. Li and Y.-F. Li, “An optimized phase-shift modulation for fast transient response in a dual-active-bridge converter,” *IEEE Trans. Power Electron.*, vol. 29, no. 6, pp. 2661–2665, Jun. 2014.
- [17] B. Zhao, Q. Song, W. Liu, and Y. Sun, “Overview of dual-active- bridge isolated bidirectional DC-DC converter for high-frequency-link power-conversion system,” *IEEE Trans. Power Electron.*, vol. 29, no. 8, pp. 4091–4106, Aug. 2014.
- [18] R. P. Severns, “Topologies for three-element resonant converters,” *IEEE Trans. Power Electron.*, vol. 7, no. 1, pp. 89–98, Jan. 1992.
- [19] X. Fang, H. Hu, Z. J. Shen, and I. Batarseh, “Operation mode analysis and peak gain approximation of the LLC resonant converter,” *IEEE Trans. Power Electron.*, vol. 27, no. 4, pp. 1985–1995, Apr. 2012.
- [20] R. Beiranvand, B. Rashidian, M. R. Zolghadri, and S. M. Hossein Alavi, “A design procedure for optimizing the LLC resonant converter as a wide output range voltage source,” *IEEE Trans. Power Electron.*, vol. 27, no. 8, pp. 3749–3763, Aug. 2012.
- [21] H. Hu, X. Fang, F. Chen, Z. J. Shen, and I. Batarseh, “A modified high-efficiency LLC converter with two transformers for wide input- voltage range applications,” *IEEE Trans. Power Electron.*, vol. 28, no. 4, pp. 1946–1960, Apr. 2013.
- [22] G. Pledl, M. Tauer, and D. Buecherl, “Theory of operation, design procedure and simulation of a bidirectional LLC resonant converter for vehicular applications,” in *Proc. IEEE Veh. Power Propulsion Conf.*, 2010, pp. 1–5.
- [23] J.-H. Jung, H.-S. Kim, J.-H. Kim, M.-H. Ryu, and J.-W. Baek, “Design methodology of bidirectional CLLC resonant converter for high frequency isolation of DC distribution systems,” *IEEE Trans. Power Electron.*, vol. 28, no. 4, pp. 1741–1755, Apr. 2013.
- [24] J. Tianyang, Z. Junming, W. Xinke, S. Kuang, and W. Yousheng, “A bidirectional LLC resonant converter with automatic forward and back- ward mode transition,” *IEEE Trans. Power Electron.*, vol. 30, no. 2, pp. 757–770, Feb. 2015.